

hypercloso-Hexa(amino)hexaboranes: Structurally Related to Known hypercloso-Dodecaboranes, Metastable with Regard to Their Classical Cycloisomers

Wahid Mesbah,^[a] Meisam Soleimani,^[a] Elham Kianfar,^[a] Gertraud Geiseler,^[b] Werner Massa,^[b] Matthias Hofmann,^[c] and Armin Berndt*^[b]

Keywords: Aromaticity / Boron / Structure elucidation / Density functional calculations

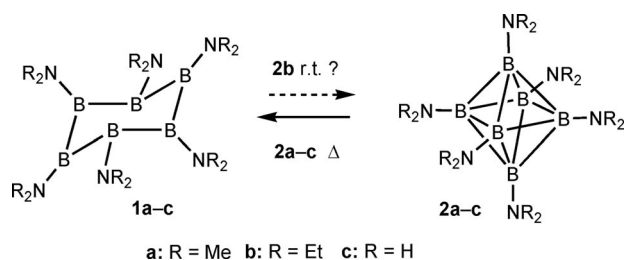
$B_6(NMe_2)_6$ (**2a**) is the first neutral *hypercloso*-hexaborane to be characterized by X-ray structural analysis. The geometry of **2a** is in nice agreement with that of the C_i symmetric molecule computed at the B3LYP/6-311+G** level of theory. Two B_3 triangles with long B...B distances in **2a** are reminiscent of those in Hawthorne's benzyloxy-substituted *hypercloso*-dodecaboranes **6a,b**. Upon heating to 200 °C, **2a** transforms into Nöth's classical cyclohexaborane **1a**. Computations at the B3LYP/6-311+G** + ZPE level of theory show **1a** to be

21.6 kcal mol⁻¹ lower in energy than **2a**, that is, the latter is metastable. *hypercloso*-Hexaborane $B_6(NEt_2)_6$ (**2b**), which was reported to be thermodynamically more stable than **1b**, is computed to be 22.4 kcal mol⁻¹ less stable than **1b**. Pure **1b** is shown here *not* to transform into **2b** upon standing in solution, which is in contrast to reports in the literature for a mixture containing **1b**.

(© Wiley-VCH Verlag GmbH & Co. KGaA, 69451 Weinheim, Germany, 2009)

Introduction

Cyclohexaborane isomer **1a** of $B_6(NMe_2)_6$ (Scheme 1) was fully characterized by the group of Nöth as early as 1980.^[1] In 1991, Baudler et al. described cyclohexaborane isomer **1b** of $B_6(NEt_2)_6$ as well as octahedral isomer **2b**, the exact geometry of which could not be determined because of disorder of the crystals.^[2] The same problem arose with **2b**, which was prepared by the group of Siebert by a new route.^[3] By means of **2a**, we here present the first X-ray structural characterization of a neutral *hypercloso*-hexaborane.^[4]



Scheme 1.

[a] Chemistry & Chemical Engineering Research Center of Iran P. O. Box 14335-186 Tehran, Iran

[b] Fachbereich Chemie der Universität Marburg Hans-Meerwein-Strasse, 35032 Marburg, Germany Fax: +49-6421-2828917 E-mail: berndta@staff.uni-marburg.de

[c] Anorganisch-Chemisches Institut der Universität Heidelberg Im Neuenheimer Feld 270, 69120 Heidelberg, Germany

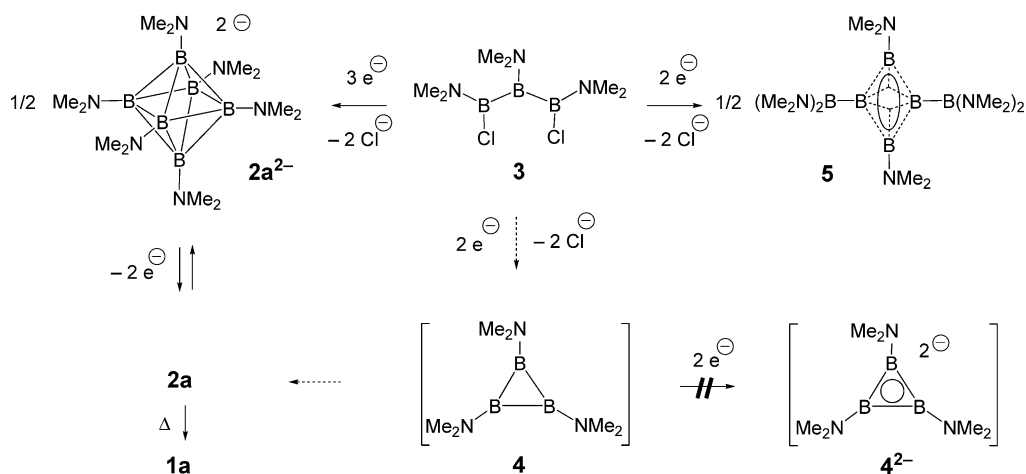
Supporting information for this article is available on the WWW under <http://dx.doi.org/10.1002/ejic.200900850>.

Cyclohexaborane **1b** has been described to spontaneously transform in solution into the “thermodynamically more stable” *hypercloso*-hexaborane **2b**.^[2] Computations for models **1c** and **2c** [i.e., $B_6(NH_2)_6$] led to inconclusive results.^[5] To clarify the contradicting reports on the relative stability of cyclic and cluster structures of neutral hexa-(amino)hexaboranes, we decided to check whether the transformation **1b** → **2b**, which had been observed with a mixture containing 68 % **1b** and a “boron-free degradation product”, can be reproduced with *pure 1b*. Computations at the B3LYP/6-311+G** + ZPE level of theory^[6] were extended to **1a–f** and **2a–f** (compare Scheme 4).

Results and Discussion

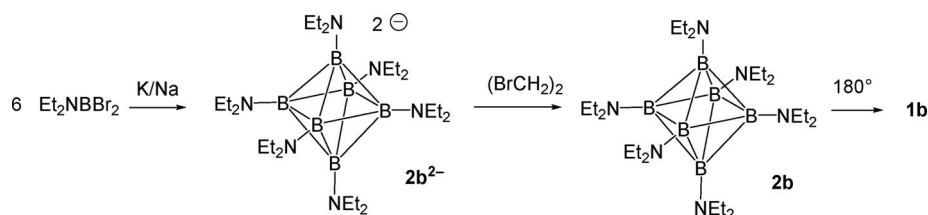
Syntheses and NMR Spectroscopic Characterization

Reaction of 1,3-dichloro-1,2,3-tris(dimethylamino)triborane(5) (**3**),^[7] with sodium/potassium alloy in pentane, with lithium powder in diethyl ether or thf at ambient temperature, or with lithium naphthalenide in thf at –100 °C did not lead to the desired cyclotriborane (triborirane) **4** or its aromatic dianion **4**²⁻, but to a 40–50 % yield of the two-electron aromatic bicyclotetraborane **5** described by Siebert et al (Scheme 2).^[8,9] Interested in the fate of the missing part of the starting material, we took a closer look at the pentane insoluble residue after workup of the reaction performed in pentane. By washing this residue with several portions of thf, we obtained a red solution of **2a**·K₂(thf)_n. Oxidation of this solution with 1,2-dibromoethane led to dark green **2a**. Compound **2a** was characterized spectroscopically by a ¹¹B chemical shift of $\delta = 41$ ppm, which is



Scheme 2

Scheme 2.



Scheme 3.

close to $\delta(^{11}\text{B}) = 40$ ppm reported for **2b**.^[2] The $\delta(^{11}\text{B}) = -14$ ppm of dianion **2a**²⁻ is in the vicinity of chemical shifts of known *closo*-hexaborane dianions ($\text{B}_6\text{H}_6^{2-}$: -13.5 ppm;^[10] $\text{B}_6\text{Cl}_6^{2-}$: -17.4 ppm^[10]). The structures of **2a**·[Li(thf)]₂ and **2a** are definitively proven by X-ray structural analyses described below.

Upon heating at 200 °C, pure **2a** cleanly transforms into orange **1a** as seen from its NMR spectroscopic data, which are in full agreement with those described by Nöth.^[1] This isomerization corresponds to the observation that crystals of **2b** transform into **1b** above 137 °C.^[2] In solution, however, cyclohexaborane **1b** was reported to isomerize spontaneously into *hypercloso*-hexaborane **2b** at room temperature.^[2]

Because computations (see below) resulted in *hypercloso*-hexa(amino)hexaboranes to be 15.1 to 22.4 kcal mol⁻¹ higher in energy than the corresponding cycloisomers, and the transformation **1b** → **2b** had been observed with a mixture containing 68% **1b** and a boron-free degradation product (“Bor-freies ... Zersetzungsprodukt”),^[2] we decided to check whether this transformation can be reproduced with pure **1b**. For this reason we synthesized **1b** by heating pure **2b** at 180 °C. The latter was obtained by oxidation of **2b**²⁻ (Scheme 3). A solution of **1b** in toluene did not change color (remained orange red) and the ¹¹B chemical shifts did not change over the course of a nine week period.

Crystal Structures

Figures 1 and 2 show the structures of **2a**·[Li(thf)]₂ and **2a**, respectively, in the crystal. Characteristic distances and

angles are compared to those computed for the isolated molecules in Table 1.

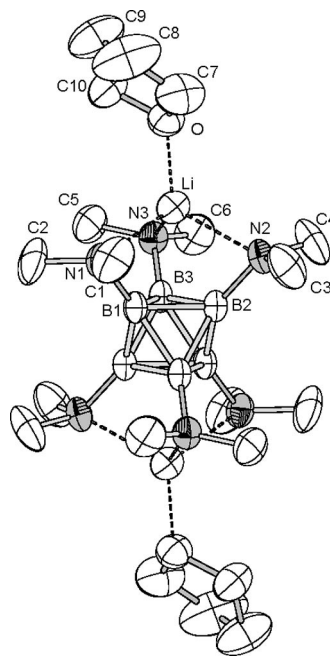


Figure 1. Structure of centrosymmetric **2a**·[Li(thf)]₂ in the crystal; hydrogen atoms are omitted for clarity. Only the more highly occupied orientation of disordered thf is shown. Displacement ellipsoids at the 50% level.

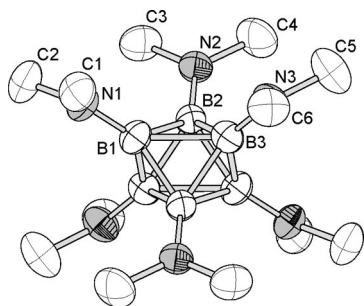


Figure 2. Structure of centrosymmetric **2a** in the crystal; hydrogen atoms are omitted for clarity. Displacement ellipsoids at the 50% level.

Table 1. Comparison of characteristic distances [pm] and angles [°] of **2a** and its dianion as determined experimentally and by computations at the B3LYP/6-311+G** level of theory. The standard uncertainties for **2a** (exp.) may be underestimated by approximately 30% due to switching off data merging for twin refinement.

| | 2a | | 2a [Li(thf)] ₂ | |
|---|-----------|-----------------------|----------------------------------|-----------------------|
| | exp. | calcd. ^[b] | exp. | calcd. ^[b] |
| B1–B2 | 188.4(2) | 185.9 | 175.1(3) | 175.0 |
| B1–B3 | 189.5(2) | 185.9 | 175.1(3) | 174.7 |
| B2–B3 | 190.1(2) | 185.8 | 175.3(2) | 175.1 |
| B1–B2 ^[a] | 171.6(2) | 170.9 | 171.7(3) | 172.2 |
| B1–B3 ^[a] | 170.7(2) | 171.0 | 172.2(3) | 172.2 |
| B2–B3 ^[a] | 169.2(2) | 171.1 | 172.1(3) | 172.1 |
| B1–N1 | 141.1(2) | 143.6 | 150.8(2) | 151.9 |
| B2–N2 | 143.4(2) | 143.6 | 151.6(2) | 151.7 |
| B3–N3 | 143.4(2) | 143.5 | 150.6(2) | 152.0 |
| B2–B1–B3 | 60.4(1) | 60.0 | 60.1(1) | 60.1 |
| B1–B2–B3 | 60.1(1) | 60.0 | 60.0(1) | 59.9 |
| B2–B3–B1 | 59.5(1) | 60.0 | 59.9(1) | 60.0 |
| B2 ^[a] –B1–B3 ^[a] | 67.5(1) | 65.8 | 61.3(1) | 61.1 |
| B1 ^[a] –B2–B3 ^[a] | 67.6(1) | 65.8 | 61.3(1) | 61.0 |
| B2 ^[a] –B3–B1 ^[a] | 67.3(1) | 65.8 | 61.1(1) | 61.1 |
| (B1,B2,B3)/B1–N1 | 35.9(1) | 36.6 | 47.3(1) | 47.3 |
| (B1,B2,B3)/B2–N2 | 36.4(1) | 36.4 | 48.5(1) | 48.2 |
| (B1,B2,B3)/B3–N3 | 36.8(1) | 36.7 | 48.2(1) | 47.3 |

[a] Symmetry operation: $-x, -y, 1 - z$. [b] Optimized at B3LYP/6-311+G**.

2a·[Li(thf)]₂ is a centrosymmetric contact ion triple of a slightly distorted octahedron **2a**²⁻ and two lithium cations, each of which coordinates a disordered thf molecule. The B···B distances of the B₃ triangles facing the lithium cations are a bit longer (175.1–175.3 pm) than those of the remaining B–B bonds (171.7–172.2 pm). On average, the B···B distances in **2a**·[Li(thf)]₂ are close (173.3 pm) to those in B₆H₆²⁻ (172.1 pm).^[10]

The B₆ nucleus of centrosymmetric **2a** may be described as a distorted octahedron or as a trigonal antiprism. Two B₃ triangles with long B···B distances (188.4–190.1 pm) are located opposite each other and connected by B–B bonds of a length (169.2–171.6 pm) close to those found in classical **1a** (172 pm on the average). The B–N bonds of **2a** are slightly longer (141.1–143.4 pm) than those in **1a** (140 pm) but considerably shorter than those in **2a**·[Li(thf)]₂ (150.6–151.6 pm). B–N bonds of length 153.9 pm have been computed for the dianion 1,6-diamino-*closo*-hexaboranate.^[11] Pyramidalization at the nitrogen centers of the substituents is considerable in **2a**·[Li(thf)]₂ [deviation of N from the B,C,C plane 39.3(2) pm, on average] but rather small in **2a** [corresponding deviation 6.8(1) pm].

Ab Initio Computations

Energies of **2a–f** and of **1a–f** (Scheme 4) were computed at the B3LYP/6-311+G** + ZPE level of theory.^[6] The energy of **1a** is 21.6 kcal mol⁻¹ lower than that of the C₇-symmetric **2a**. This is in agreement with the observed transformation of **2a** into **1a** upon heating to 200 °C. At the same level of theory, **1b** is computed to be 22.4 kcal mol⁻¹ lower in energy than **2b**.

C₇-symmetric **2c** turned out to be a minimum at the B3LYP/6-31G* level of theory, whereas D_{3d} symmetric **2c** is a minimum only at the B3LYP/6-311+G** level. The energy difference between C₇-symmetric **2c** and **1c** (15.1 kcal mol⁻¹) is close to that computed before.^[5] Classical structures of type **1** are preferred over nonclassical type **2** only when carrying strong donor substituents like amino groups. Bond lengths and angles computed for **2a** are in satisfying agreement (Table 1) with corresponding data from the X-ray crystal structure determination. ¹¹Boron chemical shifts computed at the GIAO-B3LYP/6-311+G**//B3LYP/6-311+G** level for **1a** (64.1 ppm) and **2a** (37.1, 37.4 and 38.1 ppm) are in better agreement with the experimental data of **1a** (65 ppm) and **2a** and **2b** (41 and 40 ppm) than with those computed for models **1c** (70.1 ppm) and D_{3d}-symmetric **2c** (77.2 ppm) at GIAO/HF/6-311+G(d,p)//B3LYP/6-31G(d).^[5]

Nuclear independent chemical shifts (NICS), which are widely accepted now as a measure for aromaticity and antiaromaticity,^[12] have been computed^[6] for **2a–f** and are compiled in Scheme 4. The NICS values cover a wide range from weakly aromatic (–7.5) for **2b** to strongly antiaromatic (+41.1) for **2f**. The difference between the latter NICS value

| | (R = NEt ₂) | (R = NMe ₂) | (R = NH ₂) | (R = OH) | (R = F) | (R = CH ₃) |
|--|-------------------------|-------------------------|------------------------|-----------|-----------|------------------------|
| cyclo-B ₆ R ₆ : | 1b | 1a | 1c | 1d | 1e | 1f |
| ΔE [kcal mol ⁻¹] | –22.4 | –21.6 | –15.1 | +18.0 | +31.8 | +41.0 |
| hypercloso-B ₆ R ₆ : | 2b | 2a | 2c | 2d | 2e | 2f |
| NICS: | –7.5 | –4.9 | –0.7 | +3.2 | +6.2 | +41.1 |

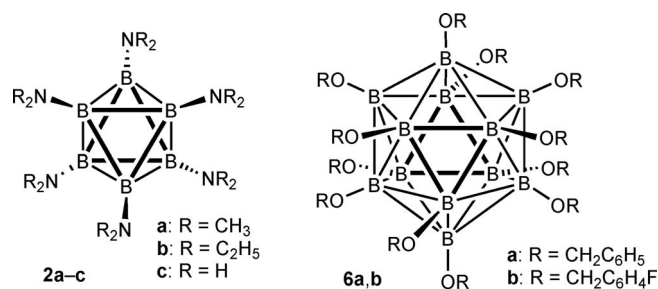
Scheme 4.

and that of aromatic $1f^{2-}$ (-26.6) is $\Delta = 67.7$ and that between $2a$ (-4.9) and $2a^{2-}$ (-32.2) only is $\Delta = 27.3$. Thus, the “gain in aromaticity” upon addition of two electrons is strongly reduced for $2a$, which owes its weak aromaticity to electrons of the donor substituents.

The strong influence of donor substituents on the NICS values of *hypercloso*-boranes has been recognized before for *hypercloso*-dodecaboranes.^[13] Aromaticity of *hypercloso*- B_4F_4 and *hypercloso*- B_9F_9 as compared to antiaromaticity of *hypercloso*- B_4H_4 and *hypercloso*- B_9H_9 has been discussed to be due to the electronegativity of the substituents.^[14]

Discussion

Geometrically, *hypercloso*-hexaborane **2a** resembles Hawthorne's *hypercloso*-dodecaboranes $B_{12}(OCH_2C_6H_4R)_{12}$ (**6a,b**),^[15] as they all contain two B_3 triangles located opposite to each other with $B\cdots B$ distances considerably longer than the remaining $B-B$ bonds of the molecules (**6a**: 191.8 vs. 175.5 ppm, $\Delta = 16.3$ pm; **6b**: 191.4 vs. 177.8 pm, $\Delta = 13.6$ pm; **2a**: 185.8 vs. 171.1 pm, $\Delta = 14.7$ pm).



Even bigger differences in $B-B$ bond lengths are computed for *hypercloso*-hexaboranes **2d**, **2e**, and **2f** ($\Delta = 24.4$, 30.9, and 27.5 pm, respectively). Bond length equalization is long known to be a characteristic of aromatics as opposed to antiaromatics, regardless of whether two- or three-dimensional aromaticity is involved.^[12,16] The reductions of the above Δ values upon increasing donor strength of the substituents may thus be taken as a hint to reduced antiaromaticity. This view is supported by the corresponding NICS values (Scheme 4), which reach from strongly antiaromatic (+41.1 for **2f**) over weakly antiaromatic (+3.2 for **2d**) to weakly aromatic (-7.5 for **2b**). Note that the NICS value computed for **2d** (3.2) is close to that of $B_{12}(OH)_{12}$ (1.3)^[13] and that both are considerably smaller than those of antiaromatic B_6Me_6 (41.1) and $B_{12}Me_{12}$ (60.1).^[13]

Our experimental finding that **1b** does not transform into **2b** is in agreement with our computed results showing **1b** to be 22.4 kcal mol⁻¹ lower in energy than **2b** but in sharp contradiction to Baudler's report on the spontaneous transformation of **1b** into **2b** in solution: “ist, ... erstmals die Umwandlung des cyclo- B_6 -Gerüsts in das oktaedrische *closo*- B_6 -Gerüst nachweisbar, die sich bei Raumtemperatur in Lösung [Kohlenwasserstoffe, (Diorganylamino)borane] durch eine allmähliche Farbänderung von orangegelb nach

olivgrün zu erkennen gibt”.^[2] A reasonable explanation for this discrepancy could be based on the fact that the reported change in color from orange-yellow to olive-green had been observed with a mixture containing 68% **1b** and a “boron-free” degradation product.^[2] The latter must be the precursor of **2b** and hence obviously cannot be “boron-free”. Its ^{11}B chemical shift must be indistinguishable from that of **1b**, that is, close to 65 ppm. Our computations for the tris(diethylamino)triborirane led to $\delta(^{11}B) = 66.7$ ppm, which is far away from $\delta(^{11}B) = 48$ ppm, as reported by Baudler. Efforts to substantiate the hypothesis outlined here are under investigation, and results will be presented in a forthcoming paper.

Experimental Section

General: Reactions were carried out under an atmosphere of dry argon or nitrogen, using standard Schlenk techniques. Solvents were dried, distilled, and saturated with nitrogen. Glassware was dried with a heat gun under high vacuum. 1H and ^{13}C NMR were recorded with a Bruker ARX 300 spectrometer, NMR references are $(CH_3)_4Si$ and $BF_3 \cdot Et_2O$. Melting points (uncorrected) were measured under an atmosphere of argon.

hypercloso-Hexakis(dimethylamino)hexaborane (2a): 1,3-Dichloro-1,2,3-tris(dimethylamino)triborane(5)^[7] (21.0 g, 89.1 mmol) was added slowly to a strongly stirred mixture of Na/K alloy (1:3, 20 mL) and pentane (300 mL) at room temperature. After heating the mixture at reflux for 10 h and cooling to room temperature, the excess amount of Na/K alloy and the produced salts (NaCl/KCl) were filtered off through a reversed frit and washed with pentane (500 mL). The brown pentane solution contained aromatic bicycloborane(4) **5**.^[8,9] Extraction of the mixture of the Na/K alloy and salts with portions of thf (400 mL in total) led to a dark red solution of *closo*- $[B_6(NMe_2)_6]K_2$. This solution was oxidized at room temperature by slowly adding 1,2-dibromoethane (4.0 g). The color of the solution immediately changed from red to black and stirring was continued for an additional hour. The solvent was then removed in vacuo and the solid black residue was digested with pentane (200 mL). The formed salts (NaBr/KBr) were filtered off through a reversed frit and washed with pentane (2×20 mL). The combined filtrates were reduced to dryness in vacuo and thoroughly dried thereafter. The deep black solid reduce of *hypercloso*- $[B_6(NMe_2)_6]$ was of almost spectroscopic purity and could be crystallized from pentane at $-30^\circ C$. Yield: 7.35 g (50%) of black solid **2a**, m.p. $>200^\circ C$ under conversion into **1a**. ^{11}B NMR (96 MHz, $[D_8]thf$, $25^\circ C$): $\delta = 41$ ppm. 1H NMR (300 MHz, $[D_8]thf$, $25^\circ C$): $\delta = 2.88$ (s, in all 36 H, NMe_2) ppm. ^{13}C NMR (75 MHz, $[D_8]thf$, $25^\circ C$): $\delta = 45.4$ (q, in all 12 C, NMe_2) ppm. White solid bicycloborane(4) **5** was obtained from the above-mentioned first pentane solution. Yield: 6.92 g (47%); for NMR spectroscopic data see ref.^[8,9]

Dilithium-closo-Hexakis(dimethylamino)hexaborate $\{2a \cdot [Li(thf)]_2\}$: 1,3-Dichloro-1,2,3-tris(dimethylamino)triborane(5)^[7] (**3**; 2.0 g, 8.5 mmol) was added slowly by syringe to a stirred suspension of lithium powder (0.3 g, 43.2 mmol) in thf (30 mL) at room temperature. The mixture turned orange red after 1.5 h. The solvent was removed in vacuo, and the solid orange residue was digested with pentane (20 mL). The excess amount of lithium powder and the formed LiCl were filtered off through a reversed frit. The orange red pentane solution was concentrated in vacuo to 5 mL and mixed with thf (ca. 2 mL). A mixture of **2a**· $[Li(thf)]_2$ and **5**^[8,9] crystallized

overnight at $-30\text{ }^{\circ}\text{C}$. Colorless platelets of **2a**·[Li(thf)]₂ (ca. 60%) and colorless needles of **5** (ca. 40%) could be distinguished and separated under the microscope. The above-mentioned solution of **2a**·K₂(thf)_n was evaporated to dryness in vacuo and the yellow residue dissolved in [D₈]thf. The NMR spectroscopic data observed were very similar to those of **2a**·[Li(thf)]₂. Data for **2a**·[Li(thf)]₂: ¹B NMR (96 MHz, [D₈]thf, 25 $^{\circ}\text{C}$): $\delta = -14$ ppm. ¹H NMR (300 MHz, [D₈]thf, 25 $^{\circ}\text{C}$): $\delta = 2.42$ (s, in all 36 H, NMe₂) ppm. ¹³C NMR (75 MHz, [D₈]thf, 25 $^{\circ}\text{C}$): $\delta = 50.1$ (q, in all 12C, NMe₂) ppm.

hypercloso-Hexakis(diethylamino)hexaborane (2b) and Cyclohexakis(diethylamino)hexaborane (1b): Dibromo(diethylamino)borane Et₂NBBr₂ (14.0 g, 57.6 mmol) was added slowly to a strongly stirred mixture of Na/K alloy (1:3, ca. 15 mL, ca. 10.8 g) and *n*-hexane (200 mL) at room temperature. After heating the mixture for 1 h at reflux and cooling to room temperature, the excess amount of Na/K alloy and the insoluble products (including NaBr and KBr) were filtered off through a reversed frit and washed with *n*-hexane (200 mL). Extraction of this mixture with portions of thf (200 mL in total) led to a dark red brown solution of sodium and potassium salts of *closo*-[B₆(NET₂)₆]²⁻ (**2b**²⁻) as characterized by $\delta(^{11}\text{B}) = -12.5$ ppm. This solution was oxidized at room temperature by slowly adding 1,2-dibromoethane (1.0 g). The color of the solution immediately changed from dark red brown to dark green. Stirring was continued for an additional hour, the solvent was removed in vacuo, and the solid black residue was digested with *n*-hexane (50 mL). Insoluble salts (NaBr/KBr) were filtered off through a reversed frit and washed with *n*-hexane (2 \times 10 mL). The combined filtrates were reduced to dryness in vacuo. The deep black solid residue of spectroscopically almost pure *hypercloso*-[B₆(NET₂)₆] (**2b**) was crystallized from *n*-hexane at $-20\text{ }^{\circ}\text{C}$ to yield 1.3 g (27%) of black solid **2b** [¹¹B NMR (96 MHz, C₆D₆, 25 $^{\circ}\text{C}$): $\delta = 40$ ppm]. Upon melting, **2b** (ca. 180 $^{\circ}\text{C}$) cleanly transformed into **1b** [¹¹B NMR (96 MHz, C₆D₆, 25 $^{\circ}\text{C}$): $\delta = 64$ ppm]. A solution of **1b** in toluene does not show any change in color and chemical shift upon monitoring by ¹¹B NMR spectroscopy over nine weeks.

X-ray Crystal Structure Analyses of 2a·[Li(thf)]₂ and 2a: Single crystals were grown from pentane at $-30\text{ }^{\circ}\text{C}$ (for **2a**) or from pentane/thf (3:1) at $-30\text{ }^{\circ}\text{C}$ [for **2a**·[Li(thf)]₂]. These crystals were investigated on area detector systems (IPDS Stoe) by using graphite monochromated Mo-*K*_α radiation at 193 K, no absorption corrections were applied. The crystal of **2a** proved to be a (001) reflection twin. After refinement of the orientation matrices of both individuals, twin integration by using combined profiles for overlapping reflections was performed.^[17] Both structures have the centrosymmetric triclinic space group *P* $\bar{1}$. The structures were solved by direct methods and difference Fourier techniques and refined against all *F*² data using full-matrix least-squares methods (SHELX programs^[18]), that of **2a** as twin. In both structures, the hydrogen atoms of the methyl groups were calculated and the torsion around the N–C bond was refined. For them isotropic displacement factors taken as 1.5 times the *U*_{eq} value of the corresponding C atom were used. In **2a**·[Li(thf)]₂ the thf molecules showed disorder over two positions with common O atom in the ratio 0.676(7)/0.324. The hydrogen atoms were kept riding in calculated positions with isotropic displacement factors set 1.2 times *U*_{eq} of their C atoms. For all heavier atoms anisotropic displacement parameters were used. Details of the experimental and crystal data are summarized in Table 2. CCDC-741779 (for **2a**) and -741778 {for **2a**·[Li(thf)]₂} contain the supplementary crystallographic data for this paper. These data can be obtained free of charge from The Cambridge Crystallographic Data Centre via www.ccdc.cam.ac.uk/data_request/cif.

Table 2. Crystal and experimental data for the structure determinations of **2a** and **2a**·[Li(thf)]₂.

| | 2a | 2a ·[Li(thf)] ₂ |
|--|---|--|
| Empirical formula | C ₁₂ H ₃₆ B ₆ N ₆ | C ₂₀ H ₅₂ B ₆ Li ₂ N ₆ O ₂ |
| Formula weight | 329.33 | 487.42 |
| Measuring temperature [K] | 193 | 193 |
| Crystal system | triclinic | triclinic |
| Space group | <i>P</i> $\bar{1}$ | <i>P</i> $\bar{1}$ |
| <i>a</i> [pm] | 744.6(2) | 907.7(1) |
| <i>b</i> [pm] | 911.0(2) | 926.8(1) |
| <i>c</i> [pm] | 926.6(2) | 1051.6(1) |
| α [°] | 61.26(2) | 92.83(1) |
| β [°] | 81.18(2) | 111.55(1) |
| γ [°] | 74.85(2) | 107.00(1) |
| Volume [Å ³] | 531.7(2) | 774.6(1) |
| <i>Z</i> | 1 | 1 |
| Calculated density [g cm ⁻³] | 1.029 | 1.045 |
| μ [mm ⁻¹] | 0.060 | 0.063 |
| <i>F</i> (000) | 180 | 266 |
| Crystal size [mm] | 0.50 \times 0.15 \times 0.05 | 0.55 \times 0.40 \times 0.25 |
| θ_{max} [°] | 26.23 | 25.90 |
| Index range | –9/9, –11/11, –11/11 | –11/11, –11/11, –12/12 |
| Scan type | ω -scans | ω -scans |
| No. of reflections | 5936 | 6193 |
| Unique refl. (<i>R</i> _{int}) | 1988 ^[a] | 2800 (0.037) |
| Observed refl. [<i>I</i> > 2 σ (<i>I</i>)] | 1476 | 1694 |
| Parameters, data/param. ratio | 116, 17.1 ^[a] | 200, 14.0 |
| Goodness-of-fit (<i>F</i> ²) | 1.196 | 0.912 |
| <i>R</i> [<i>I</i> > 2 σ (<i>I</i>)] | 0.0575 | 0.0493 |
| <i>wR</i> ₂ (all refl.) | 0.1248 | 0.1418 |
| largest diff. peak/hole [e Å ⁻³] | +0.234/–0.169 | +0.158/–0.160 |

[a] Twin refinement, reflections not merged, estimated standard deviations underestimated.

Supporting Information (see footnote on the first page of this article): Cartesian coordinates and absolute energies of structures optimized at the B3LYP/6-311+G** level of density functional theory.

Acknowledgments

This work was supported by the Deutsche Forschungsgemeinschaft (FSP Polyeder) and the Fonds der Chemischen Industrie.

- [1] H. Nöth, H. Pommerening, *Angew. Chem.* **1980**, 92, 481–482; *Angew. Chem. Int. Ed. Engl.* **1980**, 19, 482.
- [2] M. Baudler, K. Rockstein, W. Oehlert, *Chem. Ber.* **1991**, 124, 1149–1152.
- [3] W. Siebert, C.-J. Maier, P. Greiwe, M. J. Bayer, M. Hofmann, H. Pritzkow, *Pure Appl. Chem.* **2003**, 75, 1277–1286.
- [4] For crystal structures of anionic *closo*-hexaboranes, see: V. Lorenzen, W. Preetz, *Z. Naturforsch., Teil B* **1997**, 52, 565–572, and literature cited therein.
- [5] M. L. McKee, *Inorg. Chem.* **1999**, 38, 321–330.
- [6] Unless noted otherwise, structures were optimized at the B3LYP/6-311+G** level and relative energies include unscaled zero-point vibrational energy corrections from frequency calculations at the same level. ¹¹B NMR chemical shift and NICS values were derived from GIAO-B3LYP/6-311+G** computations. Gaussian 03 was employed throughout: M. J. Frisch, G. W. Trucks, H. B. Schlegel, G. E. Scuseria, M. A. Robb, J. R. Cheeseman, J. A. Montgomery Jr., T. Vreven, K. N. Kudin, J. C. Burant, J. M. Millam, S. S. Iyengar, J. Tomasi, V. Barone, B. Mennucci, M. Cossi, G. Scalmani, N. Rega, G. A. Petersson, H. Nakatsuji, M. Hada, M. Ehara, K. Toyota, R. Fukuda, J. Hasegawa, M. Ishida, T. Nakajima, Y. Honda, O. Kitao, H. Nakai, M. Klene, X. Li, J. E. Knox, H. P. Hratchian, J. B.

- Cross, C. Adamo, J. Jaramillo, R. Gomperts, R. E. Stratmann, O. Yazyev, A. J. Austin, R. Cammi, C. Pomelli, J. W. Ochterski, P. Y. Ayala, K. Morokuma, G. A. Voth, P. Salvador, J. J. Dannenberg, V. G. Zakrzewski, S. Dapprich, A. D. Daniels, M. C. Strain, O. Farkas, D. K. Malick, A. D. Rabuck, K. Raghavachari, J. B. Foresman, J. V. Ortiz, Q. Cui, A. G. Baboul, S. Clifford, J. Cioslowski, B. B. Stefanov, G. Liu, A. Liashenko, P. Piskorz, I. Komaromi, R. L. Martin, D. J. Fox, T. Keith, M. A. Al-Laham, C. Y. Peng, A. Nanayakkara, M. Challacombe, P. M. W. Gill, B. Johnson, W. Chen, M. W. Wong, C. Gonzalez, J. A. Pople, *Gaussian 03*, revision B.03, Gaussian, Inc., Pittsburgh, PA, **2003**.
- [7] G. Linti, D. Loderer, H. Nöth, K. Polborn, W. Rattay, *Chem. Ber.* **1994**, *127*, 1909–1922.
- [8] A. Maier, M. Hofmann, H. Pritzkow, W. Siebert, *Angew. Chem.* **2002**, *114*, 1600–1602; *Angew. Chem. Int. Ed.* **2002**, *41*, 1529–1532; see also ref. 16 in ref.^[9a]
- [9] a) C. Präsang, M. Hofmann, G. Geiseler, W. Massa, A. Berndt, *Angew. Chem.* **2002**, *114*, 1597–1599; *Angew. Chem. Int. Ed.* **2002**, *41*, 1526–1529; b) for the dianion of **5**, see: W. Mesbah, C. Präsang, M. Hofmann, G. Geiseler, W. Massa, A. Berndt, *Angew. Chem.* **2003**, *115*, 1758–1760; *Angew. Chem. Int. Ed.* **2003**, *42*, 1717–1719.
- [10] W. Preetz, J. Fritze, *Z. Naturforsch., Teil B* **1984**, *39*, 1472–1477, and references cited therein.
- [11] M. M. Balakrishnarajan, R. Hoffmann, *Angew. Chem.* **2003**, *115*, 3907–3911; *Angew. Chem. Int. Ed.* **2003**, *42*, 3777–3781.
- [12] Z. Chen, C. S. Wannere, C. Corminboeuf, R. Puchta, P. von R. Schleyer, *Chem. Rev.* **2005**, *105*, 3842–3888; H. Fallah-Bagher-Shaidaei, C. S. Wannere, C. Corminboeuf, R. Puchta, P. von R. Schleyer, *Org. Lett.* **2006**, *8*, 863–866, and references cited therein.
- [13] M. L. McKee, *Inorg. Chem.* **2002**, *41*, 1299–1305 and references cited therein.
- [14] R. B. King, P. von R. Schleyer in *Molecular Clusters of the Main Group Elements* (Eds.: M. Driess, H. Nöth), Wiley **2004**, pp. 1–33, especially pp. 29–30.
- [15] T. Peymann, C. B. Knobler, S. I. Khan, M. F. Hawthorne, *Angew. Chem.* **2001**, *113*, 1713–1715; *Angew. Chem. Int. Ed.* **2001**, *40*, 1664–1667; O. K. Farha, R. L. Julius, M. W. Lee, R. E. Huertas, C. B. Knobler, M. F. Hawthorne, *J. Am. Chem. Soc.* **2005**, *127*, 18243–18251.
- [16] P. von R. Schleyer, G. Subramanian, H. Jiao, K. Najafian, M. Hofmann in *Advances in Boron Chemistry* (Ed.: W. Siebert): Royal Society of Chemistry, Cambridge, UK, **1997**, pp. 3–14.; P. von R. Schleyer, K. Najafian, “Are Polyhedral Boranes, Carboranes, and Carbocations Aromatic?” in *The Borane, Carborane, Carbocation Continuum*, Wiley, New York, **1998**, pp. 169–190.
- [17] F. Hahn, *INTEGRATE^{TWIN} in XAREA 1.0*, Stoe & Cie., Darmstadt, Germany, **2005**.
- [18] G. M. Sheldrick, *SHELXS-97, Program for the Solution of Crystal Structures*, University of Göttingen, Germany, **1997**; G. M. Sheldrick, *SHELXL-97, Program for Refinement of Crystal Structures*, University of Göttingen, Germany, **1997**.

Received: August 28, 2009

Published Online: November 13, 2009